Research Article

Contribution of synergetic control to the minimization of harmonics currents injected for grid connected photovoltaic systems

Mathieu Jean Pierre Pesdjock[1,2] · Justin Roger Mboupda Pone[2] · Godpromesse Kenne[2] · Lionel Leroy Sonfack[1,2]

Received: 27 February 2020 / Accepted: 19 June 2020 / Published online: 17 July 2020
© Springer Nature Switzerland AG 2020

Abstract
This paper presents a new synergetic control scheme for grid-connected photovoltaic (PV) systems. The proposed control scheme improves the quality of energy injected by the PV inverter into the grid by minimizing the total harmonic distortion (THD) of currents during low sunlight conditions. The proposed technique makes use of an intermediate virtual control to design the new synergetic control law which is applied on a grid-connected PV system supplying linear and non-linear loads. The effectiveness of the control scheme is simulated in Matlab/Simulink software. A comparison of simulation results with other linear and nonlinear control techniques in the literature show the effectiveness, superiority and satisfactory performance of the proposed scheme in minimizing the harmonics and THD of the currents under low solar irradiance. The results also show that the proposed synergetic controller is robust and has better dynamic performance under varying irradiance conditions.

Keywords PV systems · Inverter · Total harmonic distortion · Synergetic control · Energy enhancement

1 Introduction

The use of static converters has led to the development of new control techniques for regulation and control of electrical power systems. Most of these control schemes use mathematical theories, hypotheses and physical laws to improve the performance indicators of electric power systems such as robustness, precision, and fidelity. Despite this improvement in performance, a grid-connected PV inverter produces high harmonic currents when operated under light load conditions due to low solar irradiance or non-linear loads[1]. A strong presence and/or high power demand for non-linear loads also increases harmonic problems[2]. These harmonics are highly responsible for cable heating, losses in semiconductor converters, capacitor breakdown, increased line losses, power factor degradation, vibration and acoustic noise, measurement device malfunction, line aging and unbalance voltage just to name a few[12]. These adverse effects have an impact on the quality of the energy injected into the power grid. Several control schemes have been proposed and developed in the literature to remedy the problems caused by harmonics. Some of these schemes are based on selective harmonic elimination techniques[5, 9] which aim at selecting and removing harmful harmonics from the frequency spectrum, thus minimizing THD. The major disadvantage of these solutions lie in the exact calculation of the switching angles. Also, the complexity of these algorithms reduces their feasibility. A better alternative to the selective harmonic elimination techniques is the reactive power compensation methods and algorithms[8]. These methods make use of active filters to ensure a better energy transit while canceling the reactive power produced in the network. The power quality in this case respects

✉ Justin Roger Mboupda Pone, mboupdapone00@gmail.com | [1]Unité de Recherche d'Automatique et Informatique Appliquée (UR-AIA), Department of Electrical Engineering, IUT FV of Bandjoun, University of Dschang, P.O.Box 134, Bandjoun, Cameroon. [2]Unité de Recherche de Matière Condensensée, d'Électronique et Traitement du Signal (UR-MACETS), Department of Physics, Faculty of Sciences, University of Dschang, P.O.Box 67, Dschang, Cameroon.

the standards. However, the use of these techniques for power quality improvement is often very cumbersome and expensive. Other methods consist of increasing the number of switching cells in the converters, thus allowing them to have a multi-level wave with a minimal total harmonic distortion[14]. However, they require a large number of switches which makes them also expensive and cumbersome. Many linear and nonlinear techniques have also been proposed in the literature to reduce the effects of harmonic distortion. However, linear approaches do not always produce satisfactory results in terms of minimization of THD. Hence the aim of this work is to:

- Propose an alternative solution using new synergetic control scheme applied to a grid-connected PV system to further improve the THD of currents;
- Compare the results of the proposed method with that obtained using the control approaches in[6, 10].

The rest of the paper has the following structure: In Sect. 2, a grid-connected PV systems is described. The design procedure of the proposed control scheme together with a block diagram is developed in Sect. 3. In Sect. 4, numerical simulation results are presented. Finally in Sect. 5, some concluding remarks and future perspectives end the paper.

2 Description of the grid-connected photovoltaic model

The grid-connected photovoltaic system studied in this work is derived from the works of[3, 6, 10] and its synoptic diagram is shown in Fig. 1. The diagram consists of five groups of blocks. In the first group of blocks, the photovoltaic source (PV block) is connected to a boost converter (DC/DC block). The Maximum Power Point Tracking (MPPT block) and Proportional Integral (PI block) controllers optimize the parameters of the PV block through the DC/DC block. In the second group of blocks, the C_{dc} capacitor is used for filtering the V_{dc} voltage at the input of the inverter (DC/AC block). The inverter then injects a three-phase current into the grid and the Pulse Width Modulation (PWM block). The third group consists of the R_f and L_f elements which filter the current harmonics injected by the inverter. The non-linear load block which is composed by the uncontrolled rectifier (AC/DC block) on the load (P_2, Q_2) and the linear load (P_1, Q_1) connected to the mains make up the fourth group. The fifth group consists of the DC link regulation block and the block describing the proposed synergetic control.

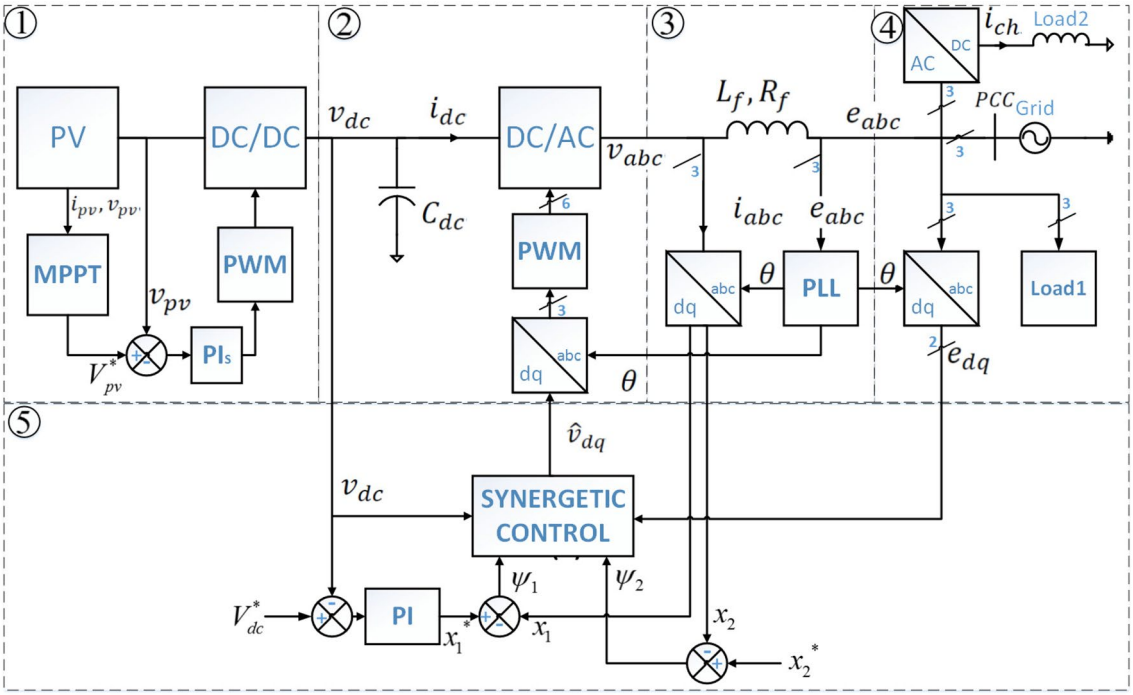

Fig. 1 Grid-connected photovoltaic system

3 Design of control strategy

The DC/DC stage of the photovoltaic system in Fig. 1 is used to keep the DC link voltage constant. This is achieved using the control strategy developed in[10]. In[3], a MATLAB/Simulink simulation model of the control strategy with PV sources is presented. The control strategy consists of regulating the v_{pv} voltage and the i_{pv} current supplied by the solar panels through two control loops. The reference voltage V_{pv}^* of the DC/DC stage is calculated using an MPPT algorithm. This algorithm maintains the power delivered by the solar panels at its maximum according to solar irradiance and temperature conditions. The d-axis reference signal i_d^* of the inverter current is computed by the control loop of the DC link while the reference q-axis component i_q^* is set to zero. The methodology used in the determination of the PI parameters is described in[11] and the values of the gains obtained are given in "Appendix".

3.1 Synergetic control strategy

3.1.1 Synthesis of synergetic control theory

Consider the nonlinear dynamic SISO system of dimension n presented by Eq. (1) where x is the state vector of the system and u the control vector. Synthesizing a synergetic controller starts with the definition of a macro-variable, which takes into account the specifications and control constraints as given in Eq. (2)[6]

$$\frac{dx(t)}{dt} = f(x,u,t) \tag{1}$$

$$\Psi = \psi(x,t) \tag{2}$$

where Ψ is the macro-variable and $\psi(x,t)$ the objective function which is defined to evolve over the chosen domain as described in Eq. (3)[4].

$$\psi(x,t) = 0 \tag{3}$$

The characteristics of the macro-variable are chosen by the designer. The choice is based on parameters such as control objective, settling time and control limitations[6, 13]. It can be a simple linear combination of state variables which are forced to evolve in a desired way expressed by a constraint chosen by the designer as shown in Eq. (4)

$$T\dot{\psi}(x,t) + \psi(x,t) = 0,\ \ T > 0 \tag{4}$$

where the control parameter T indicates the speed of convergence of the closed-loop system in the selected domain[7].

3.2 Proposed synergetic control strategy

To design a new control law based on the work of[6], let's consider Eq. (5) which describes the dynamics of the L filter connected to the grid and the macro-variable given by Eq. (6)

$$\begin{cases} \dot{x_1} = -\tau^{-1}x_1 + \omega x_2 + \delta(v_d - e_d) \\ \dot{x_2} = -\tau^{-1}x_2 - \omega x_1 + \delta(v_q - e_q) \end{cases} \tag{5}$$

$$\psi\begin{pmatrix}\psi_1\\ \psi_2\end{pmatrix} = \begin{pmatrix}x_1^* - x_1\\ x_2^* - x_2\end{pmatrix} \tag{6}$$

where $x_1 = i_d$: d-axis current, $x_2 = i_q$: q-axis current, $\tau = \frac{L_f}{R_f}$ and $\delta = \frac{1}{L_f}$.

The implementation of the new control law is achieved in two steps.

3.2.1 Step 1: Design of an Intermediate Control Law

Considering the macro-variables defined by Eq. (6), the components of the measured currents $x = [x_1\ x_2]^T$ can be expressed as (7);

$$x\begin{pmatrix}x_1\\ x_2\end{pmatrix} = \begin{pmatrix}x_1^* - \psi_1\\ x_2^* - \psi_2\end{pmatrix} \tag{7}$$

Substituting Eq. (7) in (5) yields;

$$\begin{cases} \dot{x}_1^* - \dot{\psi}_1 = -\tau^{-1}(x_1^* - \psi_1) + \omega(x_2^* - \psi_2) + \delta(v_d - e_d) \\ \dot{x}_2^* - \dot{\psi}_2 = -\tau^{-1}(x_2^* - \psi_2) - \omega(x_1^* - \psi_1) + \delta(v_q - e_q) \end{cases} \tag{8}$$

Expanding (8) and substituting the result in Eq. (9) (derived from Eq. 4), we get Eq. (10) which allows us to group the derivatives on one side.

$$\psi = -T\dot{\psi},\quad T = [T_1\ T_2]^T > 0 \tag{9}$$

$$\begin{cases} \dot{x_1}^* - \gamma_1\dot{\psi}_1 - \omega T_2\dot{\psi}_2 = -\tau^{-1}x_1^* + \omega x_2^* + \delta(v_d - e_d) \\ \dot{x_2}^* + \omega T_1\dot{\psi}_1 - \gamma_2\dot{\psi}_2 = -\tau^{-1}x_2^* - \omega x_1^* + \delta(v_q - e_q) \end{cases} \tag{10}$$

With $\begin{bmatrix}\gamma_1\ \gamma_2\end{bmatrix}^T = \begin{bmatrix}1 - \tau^{-1}T_1\\ 1 - \tau^{-1}T_2\end{bmatrix}$

Equation (10) can be rewritten as two equations; one composed of derivatives (Eq. 11) and the other representing new current dynamics (Eq. 12).

$$\begin{cases} \dot{\xi}_1 = \dot{x_1}^* - \gamma_1\dot{\psi}_1 - \omega T_2\dot{\psi}_2 \\ \dot{\xi}_2 = \dot{x_2}^* + \omega T_1\dot{\psi}_1 - \gamma_2\dot{\psi}_2 \end{cases} \tag{11}$$

$$\begin{cases} \dot{\xi}_1 = -\tau^{-1}x_1^* + \omega x_2^* + \delta(v_d - e_d) \\ \dot{\xi}_2 = -\tau^{-1}x_2^* - \omega x_1^* + \delta(v_q - e_q) \end{cases} \tag{12}$$

In fact, we define $\xi = [\xi_1\ \xi_2]^T$ as virtual currents of zero reference control. This variable allows us to perform the design in two steps. The first step consists of solving Eq. (11) while the second step consist of designing the control law. The solution of Eq. (11) is given by Eq. (13)

$$\begin{cases} \xi_1 = \int \dot{\xi}_1 = x_1^* - \gamma_1\psi_1 - \omega T_2\psi_2 - K_{\psi_1} sat(\psi_1) \\ \xi_2 = \int \dot{\xi}_2 = x_2^* + \omega T_1\psi_1 - \gamma_2\psi_2 - K_{\psi_2} sat(\psi_2) \end{cases} \tag{13}$$

where $K_{\psi_1}, K_{\psi_2} > 0$, ξ_1 and ξ_2 are virtual currents on the d and q axis respectively. The function $sat(.)$ has been arbitrarily chosen and described by Eq. (14).

$$sat(\psi) = \begin{cases} +1 \\ \psi, \quad -1 \le \psi \le 1 \\ -1 \end{cases} \tag{14}$$

3.2.2 Step 2: Synergetic $\hat{v}_{dq}$ control law

By defining the macro-variables as in Eq. (15), whose convergence condition must be satisfied by Eq. (16) and proceeding in the same way as in step 1, we obtain the control law given by Eq. (17).

$$\vartheta \begin{pmatrix} \vartheta_1 \\ \vartheta_2 \end{pmatrix} = \begin{pmatrix} \xi_1^* - \xi_1 \\ \xi_2^* - \xi_2 \end{pmatrix} \tag{15}$$

$$T'\dot{\vartheta} + \vartheta = 0,\ T' = [T_3\ T_4]^T > 0 \tag{16}$$

$$\begin{cases} \hat{v}_d = e_d + \delta^{-1}(\frac{1}{T_3}\vartheta_1 + \dot{\xi}_1^{\ *} + \tau^{-1}x_1^* - \omega x_2^*) \\ \hat{v}_q = e_q + \delta^{-1}\left(\frac{1}{T_4}\vartheta_2 + \dot{\xi}_2^{\ *} + \tau^{-1}x_2^* + \omega x_1^*\right) \end{cases} \tag{17}$$

where $\xi_1^* = \xi_2^* = 0$ are virtual reference currents on the d and q axis respectively.

Figure 2 describes the synergetic control principle proposed for the regulation of the current injected into the grid by the PV system.

4 Results and discussion

In order to evaluate the performance of the proposed synergetic control during solar irradiance variation, numerical simulations in Matlab/Simulink were performed using the same test conditions as the PI controller proposed in[10] and the synergetic control in[6]. The parameters of the power system, PV source and controllers are given in "Appendix". The solar irradiance profile used in the simulations is shown in Fig. 3b and the resulting power injected into the grid is given in Fig. 3a. It can be seen from Fig. 4 that the THD of the currents injected into the grid by the proposed synergetic control method is significantly lower than those of the controllers proposed in[6, 10] under all solar irradiance conditions. Figures 5, 6, 7 and 8 show the zooms of the currents and harmonic spectra injected into the grid for the different irradiance values. It can be seen from these figures that the amplitudes of the harmonics above the fundamental in the currents injected into the grid by the proposed method is significantly smaller than the ones presented by the other two methods. It can also be observed from these figures that the proposed approach does not affect the harmonics of the grid voltages. A quantitative evaluation and comparison of the performance of the proposed synergetic control during solar irradiance variation was also carried out with the profile shown in Fig. 3b. The average values of the current THD collected during the various operating tests are presented in Table 1. An analysis of the results of this table indicates that the THD values obtained with the proposed controller always falls within the accepted standards no matter the variations in solar irradiance. These qualitative and quantitative results show that the proposed approach presents better performances in terms of reduction of current harmonics as compared to the works of[6, 10].

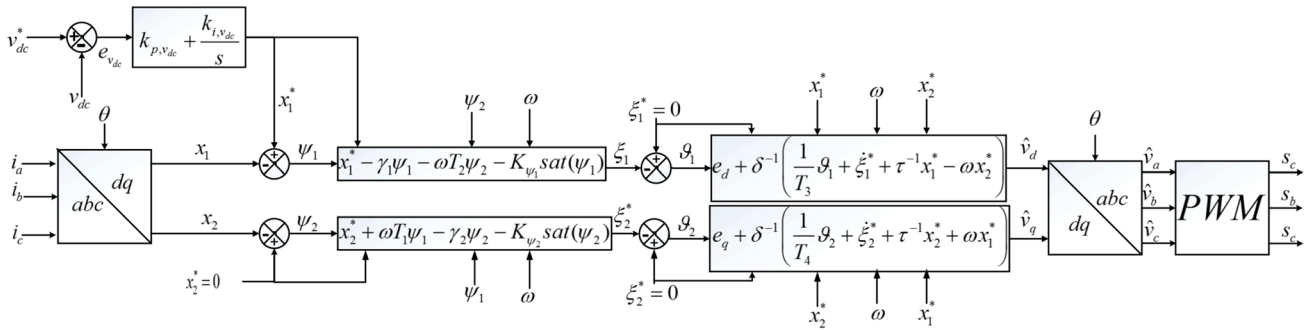

Fig. 2 Proposed synergetic control strategy

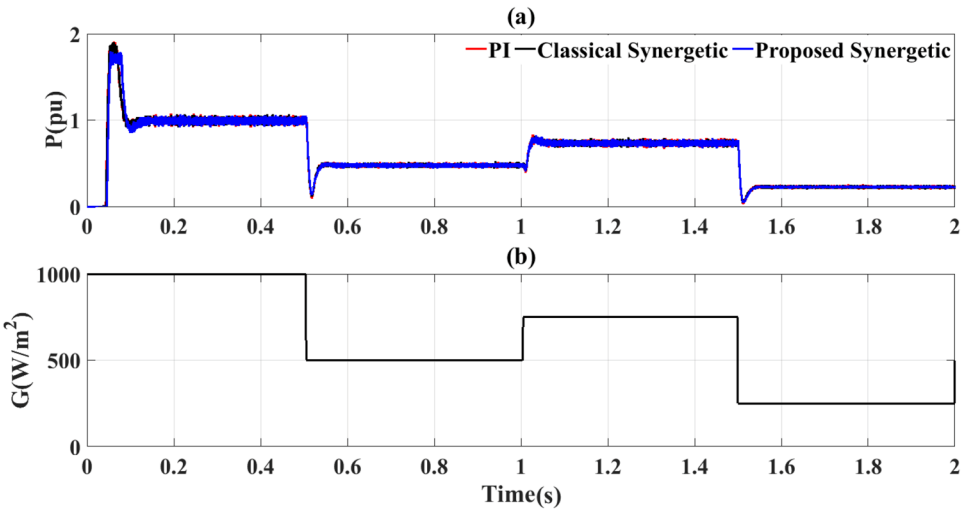

Fig. 3 System performance under varying solar irradiance conditions. **a** Power transmitted by the PV system. **b** Irradiation

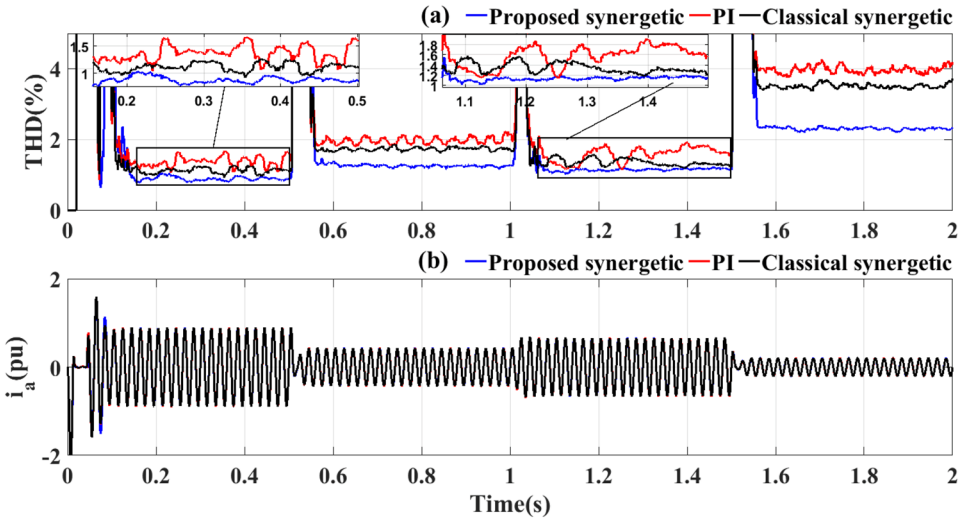

Fig. 4 System performance under varying solar irradiance conditions Fig. 3b. **a** Injected grid current THD and **b** injected current

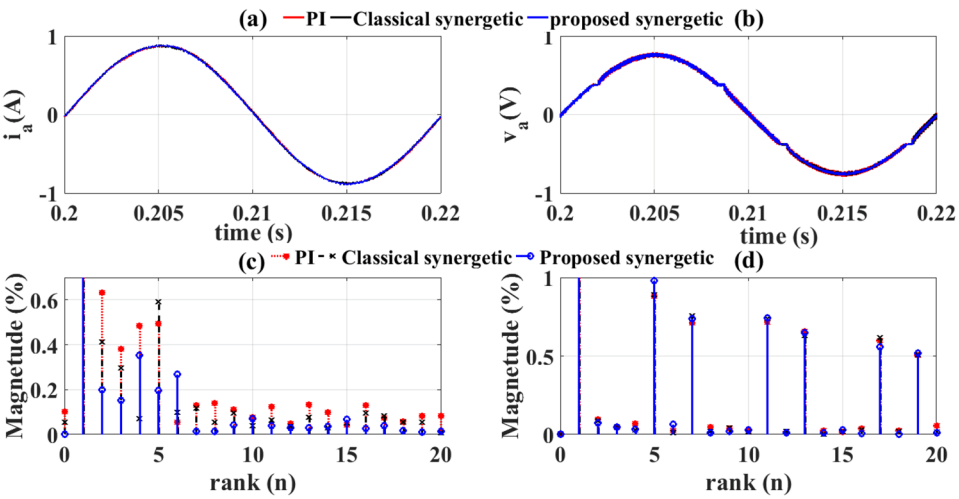

Fig. 5 Zoom of harmonic spectrum (in red: PI, in black: classical synergetic control, in blue: proposed synergetic control) at 1000 W/m^2. **a** Zoom of current flowing through phase a. **b** Zoom of voltage of phase a. **c** Harmonic spectrum of current. **d** Harmonic spectrum of voltage

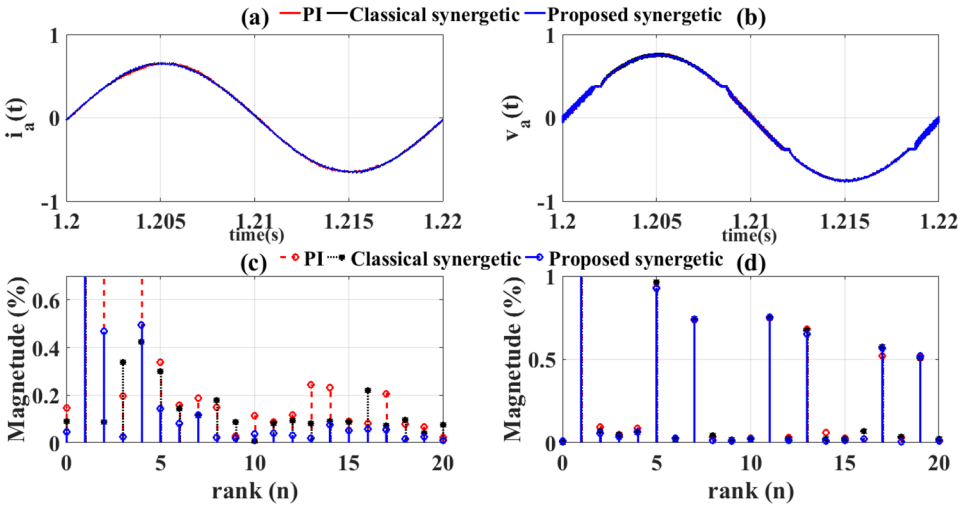

Fig. 6 Zoom of harmonic spectrum (in red: PI, in black: classical synergetic control, in blue: proposed synergetic control) at 750 W/m^2. **a** Zoom of current flowing through phase a. **b** Zoom of voltage of phase a. **c** Harmonic spectrum of current. **d** Harmonic spectrum of voltage

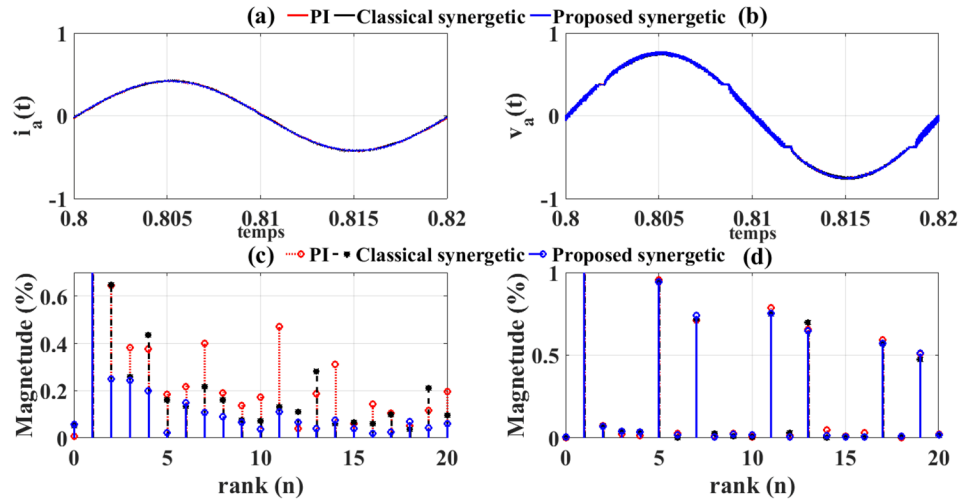

Fig. 7 Zoom of harmonic spectrum (in blue: PI, in red: classical synergetic control, in black: proposed synergetic control) at 500 W/m^2 :**a** Zoom of the current flowing through phase a. **b** Zoom of the voltage of phase a. **c** Harmonic spectrum of the current. **d** Harmonic spectrum of the voltage

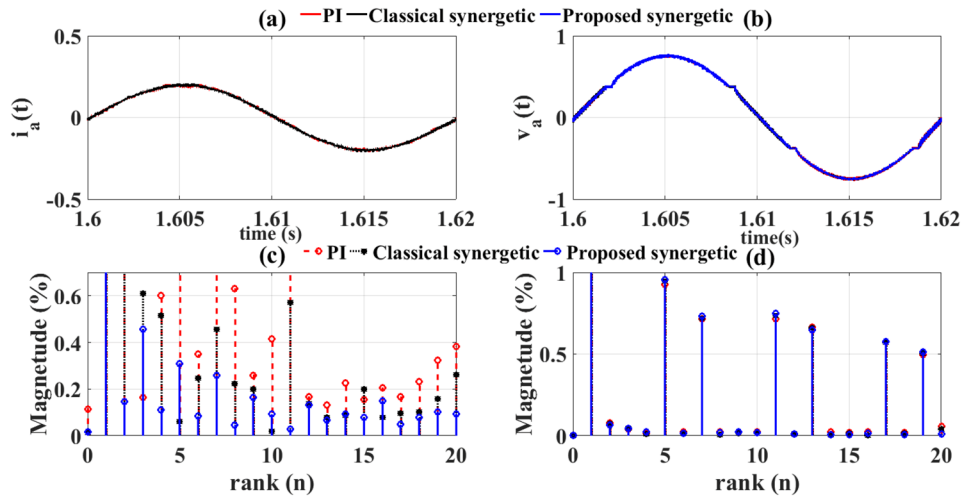

Fig. 8 Zoom of harmonic spectrum (in red: PI, in black: classical synergetic control, in blue: proposed synergetic control) at 250 W/m^2 :**a** Zoom of current flowing through phase a. **b** Zoom of voltage of phase a. **c** Harmonic spectrum of current. **d** Harmonic spectrum of voltage

Table 1 Comparative table of THD_{i_a} (%) for different solar irradiance levels

$G(W/m^2)$	1000	750	500	250
THD_{i_a}(PI)[10]	1.41	1.82	1.93	3.83
THD_{i_a}(Synergetic)[6]	1.13	1.27	1.81	3.46
THD_{i_a}(Proposed synergetic)	1.02	1.10	1.25	2.32

5 Conclusions

In this paper, a new synergetic control scheme for grid-connected photovoltaic systems is presented. The proposed control approach is robust and improved the quality of the energy injected by the PV inverter by minimizing the THD of currents during low sunlight conditions. The proposed technique made use of an intermediate virtual control which was applied to a nonlinear mathematical model of a grid-connected PV system. The effectiveness of the control scheme was verified using numerical simulations in Matlab/Simulink. A comparison of the simulation results showed the effectiveness, superiority and satisfactory performance of the proposed scheme in minimizing the harmonics and THD of the currents in the presence of nonlinear and linear loads. Our future works consist of implementing the proposed synergetic control experimentally.

Compliance with ethical standards

Conflict of interest The authors declare that they have no conflict of interest.

Appendix: simulation parameters under MATLAB/Simulink and abbreviation

See Fig. 9, Tables 2, 3, 4, 5 and 6.

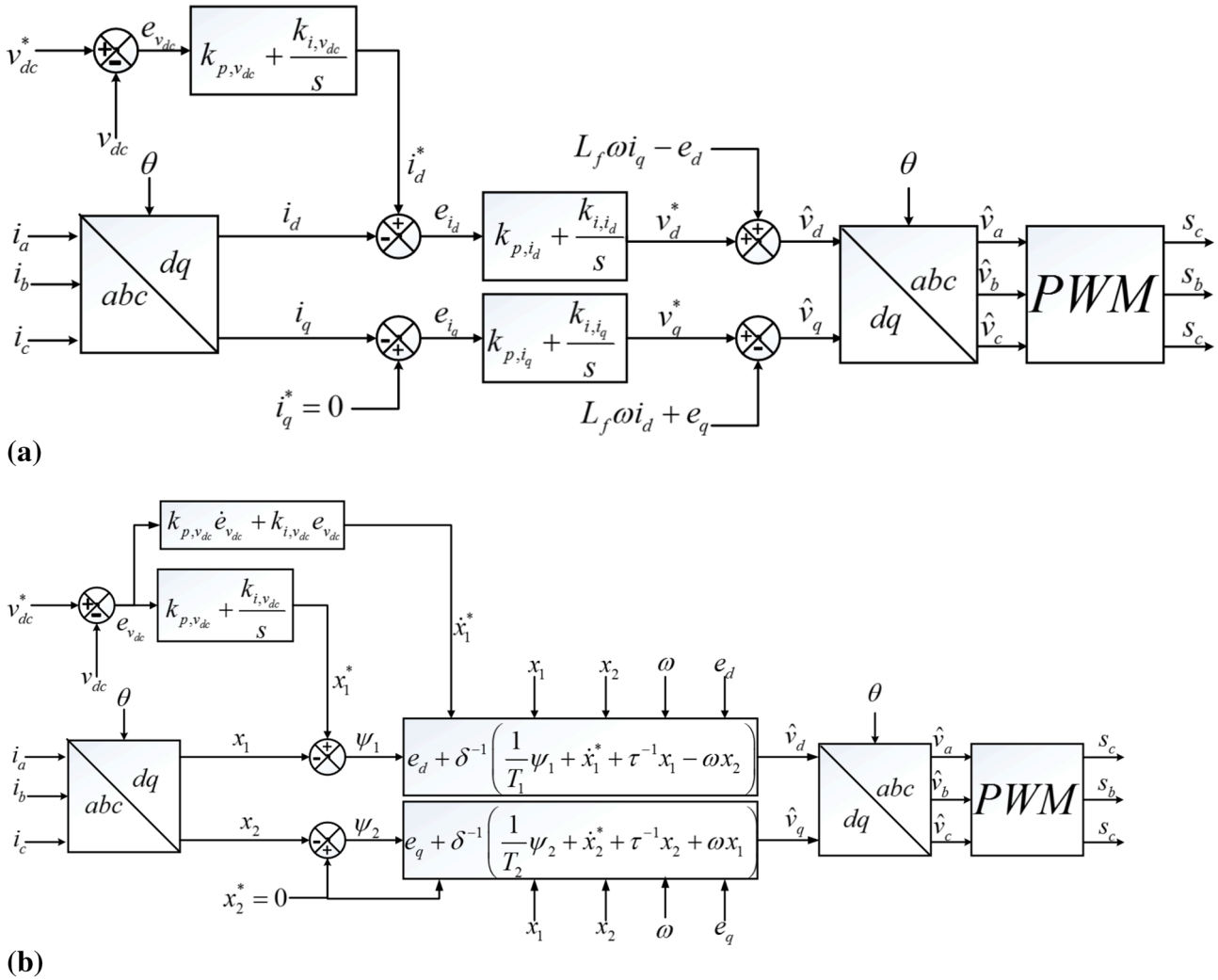

Fig. 9 Inverter control synoptic of the compared methods. **a** PI control strategy[3, 10]. **b** Classical synergetic control strategy[6]

Table 2 Synergetic control parameters

Methods	T_1	T_2	T_3	T_4	K_{ψ_1}	K_{ψ_2}
Synergetic	0.5 µs	0.5 µs	–	–	–	–
Proposed	80 µs	80 µs	1 ns	1 ns	− 18	− 18

Table 3 Power system parameters

L_f	2 mH	R_f	1 mΩ	f	50 Hz
P_1	140 kW	Q_1	2 kVar	E_a	220 V
P_2	5 kW	Q_2	1 kVar	$k_{1,d}$	0.1
V^*_{dc}	650 V	$L_{dc/dc}$	5 mH	$k_{1,q}$	0.1
$R_{dc/dc}$	5 mΩ	C_{dc}	12 mF	$k_{R_{m,dq}}$	0.1

Table 4 PV source parameters

Number of cell	96	I_{sc}	5.96 A
N_p	66	V_{0C}	64.2 V
N_s	5	V_{mp}	54.7 V
R_s	0.037 Ω	R_P	993.51 Ω
P	305 W	Total power	126.26 kW

Table 5 Controller parameters

PI regulator	k_p	k_i
DC link voltage (v_{dc})	− 3.60	− 270
d-axis current (i_d)	24	12
q-axis current (i_q)	24	12

Table 6 Abbreviations used in this paper

PV	Photovoltaïc
PI	Proportional-integral controller
THD	Total harmonics distorsion
V_{dc}	Voltage of DC link(V)
i_{dc}	Current of DC link (A)
i_{pv}, I_{pv}	Photovoltaïc array current (A)
x	State vector
v_a, v_b, v_c	Voltages at the ac bus (V)
e_a, e_b, e_c	Voltages at the ac side grid (V)
i_a, i_b, i_c	Currents injected into the ac grid (A)
L_f	Filter inductance (H)
R_f	Filter resistance (Ω)
v_{dq}	dq components of the voltage (V)
i_{dq}	dq currents injected into the grid (A)
SISO	Single input single output

References

1. Barutcu IC, Karatepe E (2017) Influence of phasor adjustment of harmonic sources on the allowable penetration level of distributed generation. Electr Power Energy Syst 87:1–15
2. Francisco GM, Raul B, Alfredo A, Maria GM, Francisco MA (2018) Power quality: scientific collaboration networks and research trends. Energies 11(8):2067. https://doi.org/10.3390/en11082067
3. Giroux P, Sybille G, Osorio C, Chandrachood S (2018) Detailed model of a 100-kw grid-connected PV array, Mathworks. Available https://www.mathworks.com/examples/simpower/mw/sps_product-power_PVarray_grid_det-detailed-model-of-a-100-kwgrid-connected-pv-array
4. Harmas M, Hamzaoui A, Harmas K, Bouchama Z (2012) Adaptive fuzzy synergetic converter control. In: 1st Taibah University international conference on computing and information technology ICCIT 2012, pp 734–738
5. Imarazene K, Chekireb H, Berkouk EM (2015) Selective harmonics elimination pwm with self-balancing dc-link in photovoltaic 7-level inverter. Turk J Electr Eng Comput Sci 24:3999–4014
6. Junjie Q, Kaiting L, Huaren W, Jianfei Y, Xiaohui L (2017) Synergetic control of grid-connected photovoltaic systems. Int J Photoenergy 2017:5051489. https://doi.org/10.1155/2017/5051489
7. Kondratiev I, Santi E, Dougal R, Veselov R (2004) Synergetic control for m-parallel connected dc–dc buck converters. In: PESC, 30th annual IEEE, vol 1, pp 182–188
8. Mamane A, Nabil A, Foulani A, Maiga S (2019) Comparative study of linear and non-linear controls of three-phase shunt active filter for improving the quality of electrical energy. Energy Power Eng 11(3):149–166
9. Mythili M, Kayalvizhi N (2013) Harmonic minimization in multilevel inverters using selective harmonic elimination pwm technique. In: Proceeding of IEEE, international conference on renewable energy and sustainable energy pp 70–74
10. Nguyen VL (2014) Couplage des systèmes photovoltaïques et des véhicules électriques au réseau: problèmes et solutions. Thèse phd, Université de Grénoble
11. Parvez M, Elias MFM, Rahim NA, Osman N (2016) Current control techniques for three-phase grid interconnection of renewable power generation systems: a review. Solar Energy 135:29–42
12. Sébastien B, Sébastien J, Jean-Charles LB, Sebastian M, Yves R, Philippe R, Guy L (2018) Improved power quality in an innovative bidirectional inverter topology. In: International conference on renewable energies and power quality, 16, vol 1, pp 193–196
13. Wang Q, Feng F, Li T (2009) Analysis of the synergetic control based on variable structure and application of power electronics. In: International Conference on Information Engineering and Computer Science, Wuhan, China, pp 9–12
14. Yaïchi M, Fellah M, Neçaibia A, Mammeri A (2011) Structure des onduleurs multiniveaux aymétriques" application aux systèmes photovoltaïque". Revue des Energies Renouvelables, pp 133–143

Publisher's Note Springer Nature remains neutral with regard to jurisdictional claims in published maps and institutional affiliations.